Available online at www.sciencedirect.com

SCIENCE DIRECT®

Journal of Catalysis 235 (2005) 295–301

JOURNAL OF CATALYSIS

www.elsevier.com/locate/jcat

An in situ XAS study of Cu/ZrO_2 catalysts under de-NO_x reaction conditions

Alfonso Caballero [*], Jose Jorge Morales, Ana Maria Cordon, Juan Pedro Holgado,
Juan Pedro Espinos, Agustin R. Gonzalez-Elipe

Departamento de Quimica Inorganica e Instituto de Ciencia de Materiales de Sevilla, Universidad de Sevilla—CSIC,
Av. Americo Vespucio s/n. 41092 Sevilla, Spain

Received 15 June 2005; revised 9 August 2005; accepted 11 August 2005

Abstract

This paper reports an X-ray absorption spectroscopy investigation of the chemical state of copper in Cu/ZrO_2 catalysts under reaction conditions. The catalysts were subjected to different treatments with hydrocarbons (CH_4, C_3H_8, or C_3H_6) and hydrocarbon/NO and hydrocarbon/NO/O_2 mixtures. The analysis was done for samples heated in situ at temperatures ranging from 298 to 773 K. The first derivative of the X-ray absorption near-edge structure (XANES) spectra of the Cu K edge was analysed by factor analysis (FA). This analysis provided an accurate means of estimating the percentages of Cu^{2+}, Cu^+, and Cu^0 under each reaction condition. Before reaction, the original catalyst consisted mainly of Cu^{2+} species. Heating the catalyst with the hydrocarbon to 573 K led to its partial reduction with formation of a significant amount of Cu^+. At the higher temperature, and depending on the hydrocarbon, Cu^0 species were dominant. When the catalyst was treated at 773 K with mixtures consisting of hydrocarbons plus NO, there was still a significant concentration of Cu^+ and Cu^0 species, although the relative concentration of Cu^{2+} generally increased. For these gas mixtures, it was also found that the relative concentration of the three different oxidation states of copper was highly dependent on the type of hydrocarbon. In general, the concentration of reduced species was related to the reactivity of the hydrocarbon ($CH_4 < C_3H_8 < C_3H_6$) and was particularly high with C_3H_6. Finally, the analysis showed that most copper remained as Cu^{2+} when the sample was heated in a hydrocarbon/NO/O_2 mixture at 773 K, although some Cu^+ can persist under these conditions. Some quantitative discrepancies were observed by comparing the results obtained by XANES/FA and those obtained by fitting analysis of the extended X-ray absorption fine structure spectra. However, the higher concentration of Cu^+ species detected by XANES/FA analysis under working conditions is congruent with temperature-programmed reduction and X-ray photoelectron spectra experiments on this sample. It is concluded that the combination of these two procedures may yield more reliable information about the physicochemical state of the different Cu^{2+}, Cu^+ and Cu^0 species existing in the Cu/ZrO_2 catalyst under de-NO_x reaction conditions.

Keywords: Cu/ZrO_2; Factor analysis; SCR; XAS; XPS; TPR; NO

1. Introduction

The selective catalytic reduction (SCR) of NO in the presence of oxygen and hydrocarbons has attracted much recent interest because of the significant environmental impact of this process [1,2]. Among the different catalyst and active phase formulations that have been proposed for this reaction, copper with zeolites or other oxide supports have been some of the most widely used options [3–5]. In these systems, a very important point of investigation is analysis of the role of copper in the catalytic reaction and, consequently, the determination of its actual chemical and coordination state under reaction conditions. Various methods, including electron spin resonance (ESR) [6], X-ray photoelectron spectroscopy (XPS) [7], Fourier transform infrared spectroscopy (FTIR) [8], and other techniques [9], have been used for this purpose. However, most of the experimental results have been obtained with after-treated samples, not during reaction conditions. X-ray absorption spectroscopy (XAS) can be applied to investigate catalysts under real working con-

---

[*] Corresponding author. Fax: +34 954460665.
E-mail address: caballero@us.es (A. Caballero).

0021-9517/$ – see front matter © 2005 Elsevier Inc. All rights reserved.
doi:10.1016/j.jcat.2005.08.008

ditions of temperature and pressure [10]. Several works have been published reporting in situ XAS analysis of Cu-ZSM5 and other related copper-containing catalysts [11–13]. In the present investigation we applied in situ XAS to ascertain the chemical state of copper in a Cu/ZrO_2 catalyst that was previously probed as active for the SCR reaction with different hydrocarbons (methane, propane, and propene) as reductive agents [7,8,14]. The work is focused primarily on the development of a simple and reliable procedure for X-ray near-edge absorption spectra (XANES) that may provide a semiquantitative estimation of the different chemical forms of copper (i.e., Cu^{2+}, Cu^{+}, and/or Cu^{0}) under different working conditions (e.g., temperature, reaction mixture) of the catalysts. The procedure developed relies on the factor analysis (FA) technique and the first derivative spectra of the XANES spectra. Using FA to deal with XANES spectra of a Cu–Pd catalyst was proposed by Fernández-Garcia et al. [15]. More recently, other publications have reported the use of this mathematical procedure in both XANES [16] and extended X-ray absorption fine structure (EXAFS) [17]. In the present investigation, we propose using the first derivative of the XANES spectra as a more reliable and simple alternative for applying the FA method. Comparing the results with those obtained from fitting analysis of the EXAFS spectra of copper under the same working conditions allows us to calculate the relative concentration of the different chemical states of copper (i.e., Cu^{0}, Cu^{+}, or Cu^{2+}) existing in the catalysts for each reaction mixture and temperature of reaction. The high stability of Cu^{+}, detected even under oxidizing conditions, has been confirmed by temperature-programmed reduction (TPR) and XPS analysis.

2. Experimental and methods

2.1. Catalyst preparation

A Cu/ZrO_2 sample (3% weight of Cu) was prepared by wetting impregnation with a $Cu(NO_3)_2$ solution of a ZrO_2 powder prepared by forced hydrolysis [18]. For the preparation of ZrO_2, a 0.2 M solution of $ZrOCl_2$ placed on a sealed beaker was heated at 363 K for 70 h, then cooled rapidly with cold water. The suspension obtained was dialysed until chlorine ions were eliminated, centrifuged, and rinsed with distilled water several times. The resulting deposit was oven-dried at 323 K for 24 h. The resulting ZrO_2 presented a specific surface area, $S_{\mathrm{BET}} = 50\ \mathrm{m^2\,g^{-1}}$, after calcination at 673 K. Once impregnated, the solid was oven-dried at 373 K for 5 h, then calcined in a 100 $\mathrm{mL\,min^{-1}}$ 3% O_2/He flow at 673 K for 3 h.

2.2. X-Ray absorption spectroscopy

XAS spectra were recorded at the BM29 beam line of the ESRF synchrotron (Grenoble, France). The spectra were acquired in transmission mode using a Specac infrared-transmission cell equipped with Kapton windows that allow in situ treatment of the sample under controlled gas mixtures and temperatures up to 773 K. The sample was placed in a stainless steel holder directly in contact with the gas mixture atmosphere and resistively heated. The samples were pressed as self-supported wafers in a standard 13-mm die, using the optimum weight to maximise the signal-to-noise ratio in the ionisation chambers. For energy calibration, a standard Cu foil introduced after the sample was measured at the same time. Typical EXAFS spectra of Cu K edge were recorded from 8800 to 10,000 eV, with a variable step energy value, with a minimum 0.5-eV step across the NEXAFS region (8970–9010 eV). EXAFS spectra were analysed using a standard package developed by Bonin et al. [19], using the theoretical amplitude and phase shift functions proposed by Rehr et al. (version 7.02 [20]). Data from the XANES region (8970–9010 eV) were normalized and derived analytically using standard algorithms, and treated without further processing.

Reference spectra for Cu^{0} and Cu^{2+} oxidation states were recorded using standard reference samples of a metallic foil and CuO powder, respectively. For the Cu^{+} oxidation state, no reference was available, but our results were compared with data in the literature [21]. Also, as shown later in this paper, a reference for Cu^{+} was obtained from mathematical analysis of the experimental spectra.

For the reaction treatments, NO, hydrocarbons (CH_4, C_3H_8, or C_3H_6) and oxygen were diluted in He (1000 ppm, 2500 ppm, and 3%, respectively). Mass flow controllers were used for dosing the gases to the cell, using a total flow of 100 $\mathrm{mL\,min^{-1}}$. The catalysts were placed in contact with the mixture at room temperature, then heated up to the desired temperature using an ascendant heating ramp of 10 $\mathrm{K\,min^{-1}}$, followed by a temperature-constant period of 1 h. Then the cell was cooled to room temperature and the spectra were recorded in contact with the reaction mixture.

2.3. Factor analysis

Analysis of the XANES spectra was performed by FA, a multivariate statistical procedure used widely in such areas as ISS, XPS, SIMS, and XAS [22,23]. This mathematical technique enables determination of the minimum number of factors (chemical components in our case) needed to reproduce the data within experimental error. A detailed description of the technique was given previously [24,25]. An important aspect of this technique is that each data point is inherently weighted in proportion to its value. This means that points with higher absolute values (i.e., intensity) will have more importance statistically than those with smaller values. This fact is specially important to take into account in spectral shapes as those found in XAS, where a jump is superimposed on features resulting from, for instance, different oxidation states. Taking the raw spectrum, this feature would mean that those points after the jump (with a higher value) would have statistically more importance than those around the edge, despite the appearance of importance features in that zone. To minimize these effects, we analysed the data of XANES region in a derivative mode, a method proposed by Okamoto et al. [26] for improving the determination of the different oxidation states in Cu K edge spectra. In addition, this method replaces the "background" removal procedure used when analysing data by some other techniques.

2.4. X-Ray photoelectron spectroscopy

XPS spectra were recorded with a Leybold-Heraeus LHS-10 spectrometer (base pressure 3×10^{10} Torr) working in the constant-pass energy mode at a value of 40 eV. The Al-K_α radiation ($h\upsilon = 1486.6$ eV) was used as excitation source. Binding energy (BE) reference was taken at the C1*s* peak of the carbon contaminating the surface of the samples at a value of 284.6 eV.

2.5. Temperature-programmed reduction

TPR was carried out in H_2/Ar flow (50 mL min^{-1}, 5 vol% H_2) from room temperature to 500 °C at a heating rate of 10 °C min^{-1}. A TCD previously calibrated with CuO was used as a detector to monitor the hydrogen consumption. The samples were previously calcined in air at 500 °C for 1 h, then cooled to room temperature.

3. Results and discussion

3.1. Cu K edge XANES spectra

Fig. 1, left, shows the Cu *K* edge spectra of the Cu/ZrO_2 catalysts recorded in situ after treatment with the indicated propene gas mixtures and temperatures. This figure clearly shows that significant changes in the shape of the spectra occurred depending on the actual chemical treatment of the sample. The most significant feature was the development of a shoulder at around 8980 eV that resulted in a shift in the position of the absorption edge of the spectra. Clearer evidence of these changes can be obtained by calculating the first derivative curves of these XANES spectra. The curves obtained are shown in Fig. 1, right, along with similar curves for CuO and Cu^0 reference samples included for comparison. The XANES spectra of CuO and Cu^0 as recorded in the same Synchrotron beamline were similar to those reported in the literature [27] for these materials and were not been included in Fig. 1, left, for the sake of simplicity. The most prominent differences between the first derivative curves appeared in the region between 8975 and 8985 eV, that is, in the zone corresponding to the moving "edge" of the integral spectra of Fig. 1.

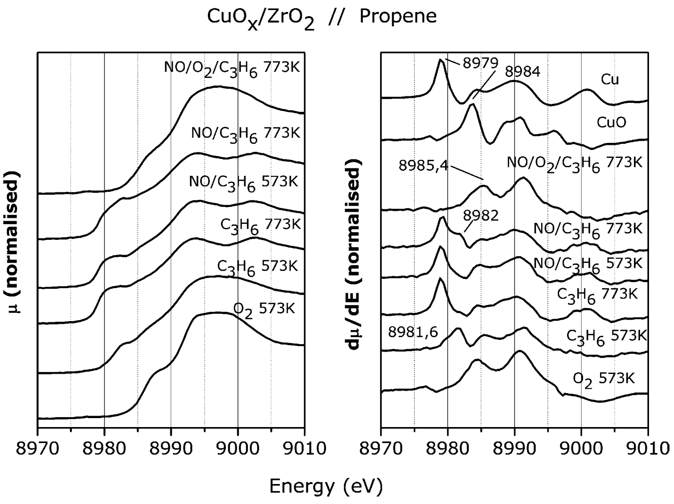

Fig. 1. (Left) Cu *K* edge XANES spectra for a Cu/ZrO_2 spectra recorded during reaction with the indicated gas mixtures containing C_3H_6 at the indicated temperatures. (Right) First derivative of the spectra of the Cu/ZrO_2 catalysts shown in the left panel. The derivative spectra of CuO and Cu are included in this figure for comparison.

First derivative curves are more sensitive than integral curves for detecting the formation of new chemical states. This is clearly evidenced by a direct comparison of the first derivative curves of the catalysts under different reaction conditions with those of the reference materials plotted in this figure. Thus, it appears that the peak at 8979 eV in the curve of metallic copper can be taken as a characteristic fingerprint of Cu^0, whereas that at 8984 eV, although existing in the curve of metallic state, is the most intense and characteristic of Cu^{2+} species. The development of peaks at these energies for the catalyst subjected to different treatments is a clear indication of the formation of these species. Thus it can be concluded that although Cu^{2+} species are predominant in the catalyst heated with O_2 at 573 K and with the $NO/O_2/C_3H_6$ mixture heated at 773 K, Cu^0 species formed in the catalyst heated with C_3H_6 at 773 K. However, the development of a peak at 8982 eV for the sample heated with C_3H_6 at 573 K and a shoulder at this position when heated with a NO/C_3H_6 mixture at 773 K do not fit the pattern of typical energy positions described for Cu^0 and CuO. This new feature can be attributed to the formation of Cu^+ species in the Cu/ZrO_2 catalysts treated under the aforementioned conditions. Fig. 1, and particularly the first derivative spectra in right, shows an easy way to perform a first assessment of the evolution of the chemical states of copper in the Cu/ZrO_2 catalysts treated under different conditions. Thus, it appears that during the treatment with O_2 at 573 K, Cu^{2+} was the predominant copper species. After heating with C_3H_6 at 573 K, most copper transformed into Cu^+, which in turn yielded Cu^0 after heating with this gas at 773 K. Then the catalyst was treated with a NO/C_3H_6 mixture to 573 K, with no changes noted in the oxidation state of copper. However, the same gas mixture at 773 K favoured the formation of Cu^+ species, demonstrating the relatively high oxidation activity of NO at this temperature. Finally, the addition of O_2 to the reaction mixture led to the oxidation of copper into Cu^{2+}, which was now the predominant species.

Similar qualitative assessments can be done for the other two experimental situations studied in this work, with C_3H_8 and CH_4 used as hydrocarbons. Figs. 2 and 3 show the results for these experiments. These two figures report the Cu *K* edge XANES spectra and their first derivative after heating the Cu/ZrO_2 catalyst with mixtures containing C_3H_8 or CH_4, respectively, together with NO and/or O_2 at 573 K and 773 K.

Depending on the hydrocarbon, differences in reactivity can be deduced by comparing Figs. 1 and 3. Thus, whereas Cu^0 species were dominant after the treatment with C_3H_6 at 773 K, the reaction with propane at the same temperature gave peaks with similar intensities, due to Cu^+ and Cu^0 species. Finally, after the treatment with CH_4 at 773 K, the derivative line was dominated by the peak at 8982 eV, due to Cu^+ species. This behaviour, related to the higher reactivity of the C_3H_6 hydrocarbon, can be observed in all of the treatments. Finally, in the

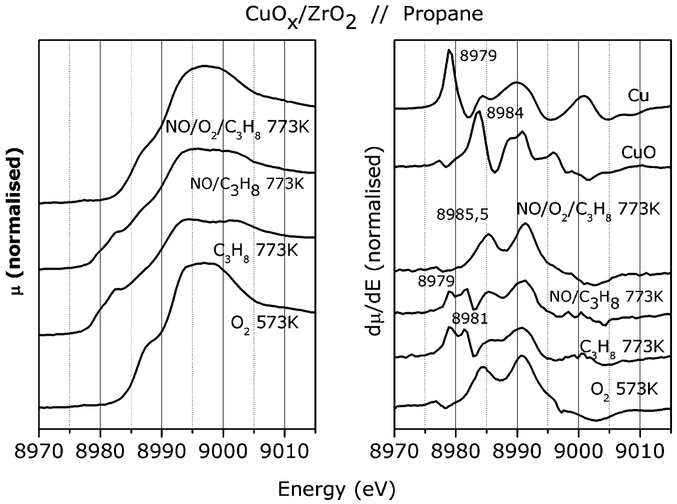

Fig. 2. (Left) Cu *K* edge XANES spectra for a Cu/ZrO$_2$ spectra recorded during reaction with the indicated gas mixtures containing C$_3$H$_8$ at the indicated temperatures. (Right) First derivative of the spectra of the Cu/ZrO$_2$ catalysts shown in the left panel. The derivative spectra of CuO and Cu are included in this figure for comparison.

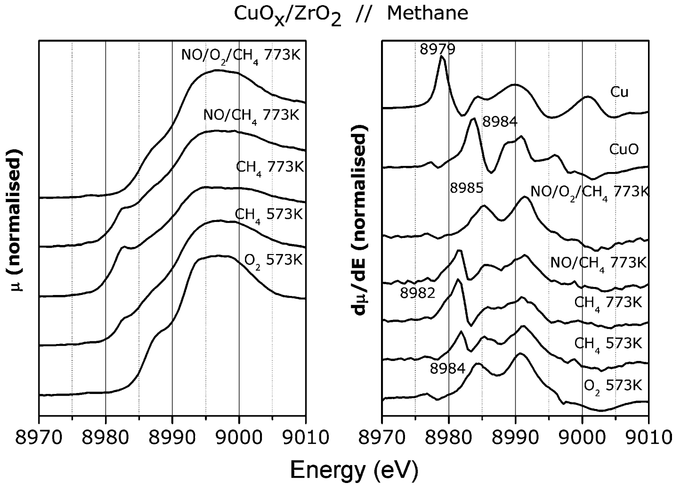

Fig. 3. (Left) Cu *K* edge XANES spectra for a Cu/ZrO$_2$ spectra recorded during reaction with the indicated gas mixtures containing CH$_4$ at the indicated temperatures. (Right) First derivative of the spectra of the Cu/ZrO$_2$ catalysts shown in the left panel. The derivative spectra of CuO and Cu are included in this figure for comparison.

presence of oxygen, whatever the hydrocarbon, Cu^{2+} species were dominant.

3.2. *Factor analysis of first derivative spectra*

A quantitative estimation of the relative concentration of each oxidation state of copper is possible by using the FA technique [22]. This procedure was previously used for the analysis of XANES spectra of Cu–Pd bimetallic catalysts [15]. By applying this mathematical procedure to the derivative spectra in Figs. 1–3 in the zone of 8972–8988 eV, we obtained that three principal components (PCs) sufficed to reproduce the shape of all experimental spectra. The shape of these three PCs, shown in Fig. 4, have been attributed to CuO (peak at 8984 eV), Cu$_2$O (peak at 8982 eV), and Cu^0 (peak at 8979 eV) species. The fact that the position of the PCs attributed to CuO and Cu^0 coincided with the experimental position found for the principal contribution of these two reference samples supports such an attribution. The partition values of each PC in each spectrum for the different gas mixtures and reaction temperatures selected are shown in Fig. 5 in the form of bar diagrams. A first evaluation of the values reported in this figure confirms the qualitative evolution of oxidation states discussed earlier for the three experiments shown in Figs. 1–3. However, the quantitative data in Fig. 5 reveal that a mixture of chemical states (Cu^0, Cu$^+$ and Cu^{2+}) are present in most experimental situations, even though a first look at some of the spectra in Figs. 1–3 does not clearly reveal the presence of more than one chemical state. Various interpretations based on the partition of given chemical states of copper have been proposed to explain the reactivity of Cu-based catalysts. Thus, it has been claimed that the formation of intermediate Cu$^+$–NO adsorbed states is critical for activation of the NO molecules [28]. According to other interpretations, a direct interaction between NO and carbonaceous species would constitute the limiting step for the reduction of NO [8,29]. Also, previous in situ XPS results from our laboratory [8] indicated that under NO reduction conditions, in contact with a hydrocarbon/NO/O$_2$ mixture, no monovalent copper species were present in the Cu/ZrO$_2$ catalytic system. However, the results in Fig. 5 indicate that Cu$^+$ species are present in almost all experimental situations, even under oxygen-rich conditions such as those existing in real exhaust streams (e.g., catalysts heated with NO/O$_2$/hydrocarbon mixtures at 773 K).

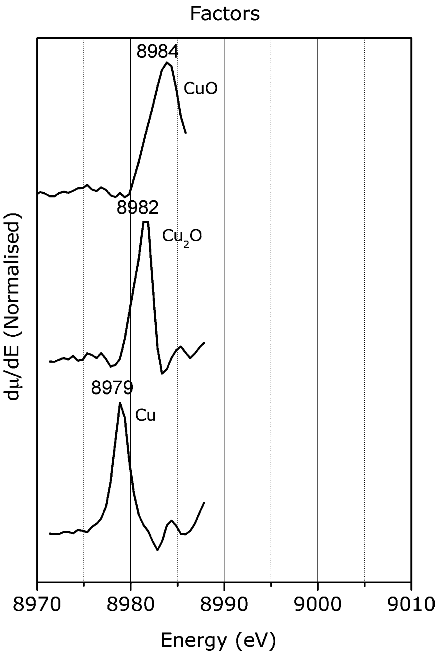

Fig. 4. Shape of PCs obtained by FA from a data base consisting of the first derivative spectra in Figs. 1–3. These PCs reproduce all the first derivative spectra in these figures. They are attributed to Cu^0, Cu$^+$ and Cu^{2+} species.

Comparing the three panels in Fig. 5, it appears that the extent of reduction to Cu$^+$ and Cu^0 states for the mixtures He/HC$_x$ and He/HC$_x$/NO (HC$_x$ = hydrocarbons such as CH$_4$,

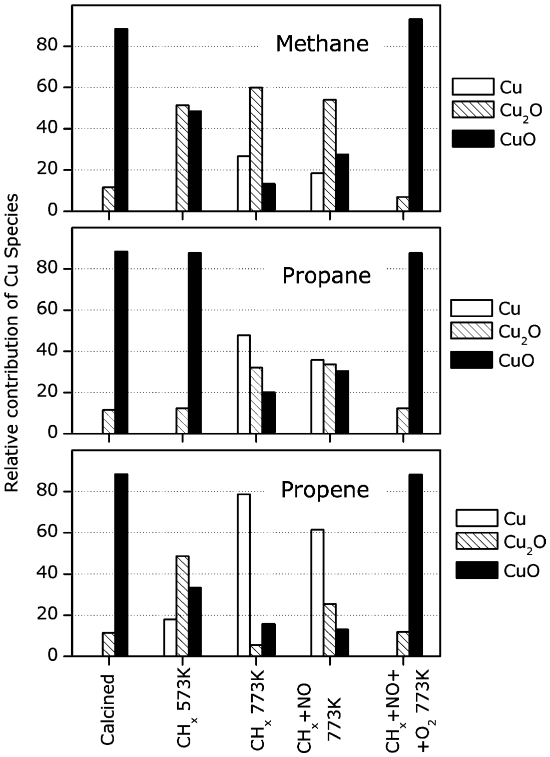

Fig. 5. Percentage of the different copper species in the Cu/ZrO$_2$ catalyst under reaction conditions determined by FA for the different experimental situations whose XANES spectra are shown in Figs. 1–3.

C_3H_6, C_3H_8) depends on the type of hydrocarbon, following the tendency $C_3H_6 > C_3H_8 > CH_4$. This trend coincides with the known reductive character of these three hydrocarbons (i.e., their tendency to dehydrogenation to yield carbon residues) and support previous results with this Cu/ZrO$_2$ catalyst [7], where XPS showed that the amount of carbon residues produced on its surface follows this reductive character.

3.3. *Cu K edge EXAFS spectra*

Studying the local structure around the copper atoms based on the analysis of the Fourier transform (FT) curves of the EXAFS spectra allow validation of the FA results reported in the previous section. Fig. 6 shows the FT curves for all of the experimental situations considered in this study. Careful observation can qualitatively detect the reduction of copper to Cu^+ and Cu^0, either by a displacement in the position of the first shell coordination peak to higher values of R or by a broadening of the peak in that direction for reaction conditions that, according to the previous XANES spectra, produces an increase in the relative concentration of Cu^+ or Cu^0 species (i.e., by heating with the hydrocarbon at 573 and 773 K and with the NO/CH_x mixture at 773 K). Table 1 summarises the best-fitting parameters that reproduce this first peak of the FT curves. Three types of bonding distances were detected from this analysis: one between 1.99 and 2.01 Å attributed to Cu^{2+}–O bonds, another at about 1.85 Å attributed to Cu^+–O bonds, and a third at 2.52 Å, close to that corresponding to Cu–Cu bonds [30].

A first assessment of the fitting parameters given in Table 1 compared with the results from XANES reproduced in Figs. 1–3 reveals good qualitative agreement, but also important quantitative differences. In fact, by fitting analysis, only Cu^{2+}–O distances could be detected after all of the treatments with oxygen mixtures at 473 or 773 K, in agreement with our previous XPS results obtained for this catalytic system [8]. However, as shown earlier, under the same conditions, about 10% of Cu^+ species were detected by FA (Fig. 5). It is noteworthy that the fitting analysis results show that this copper(II) oxide phase had a coordination number of about 3.5, lower than the value of 4 characteristic of massive CuO [30]. This fact could in principle be generically related to the existence of a distorted CuO phase dispersed over the zirconia surface. The FA results suggest an alternative explanation related to the existence of a mixture

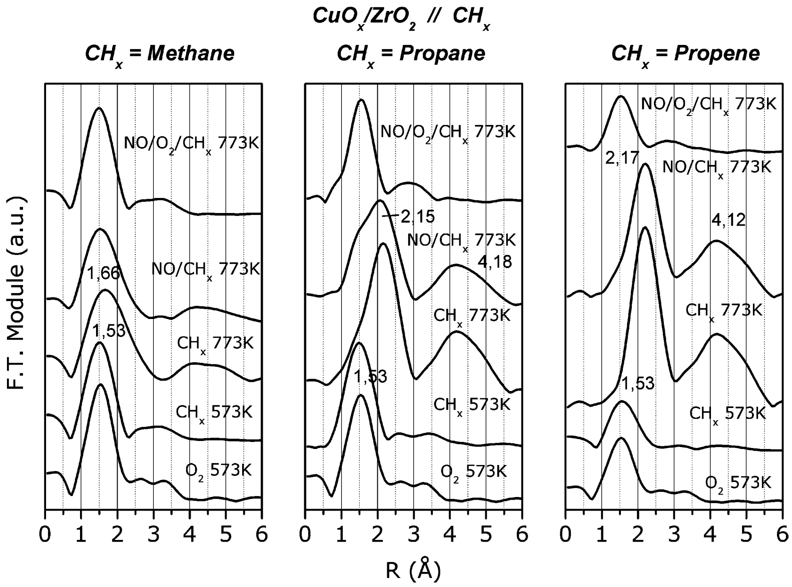

Fig. 6. FT curves of the Cu *K* edge EXAFS spectra of the Cu/ZrO$_2$ catalysts under reaction conditions as indicated in the figure. (Left) Reaction mixtures containing CH_4. (Middle) Reaction mixtures containing C_3H_8. (Right) Reaction mixtures containing C_3H_6.

Table 1
Fitting results (coordination number and radial distances) for Cu/ZrO_2 catalysts at the indicated treatments. FA corrected C.N. in parentheses

Treatment	Shells[a]	C_3H_6		C_3H_8		CH_4	
		R (Å)	C.N.	R (Å)	C.N.	R (Å)	C.N.
O_2, 573 K	Cu–O_1	1.96	3.5	1.96	3.5	1.96	3.5
C_xH_y, 573 K	Cu–O_1	1.98	1.7	1.94	3.6	1.99	1.8
	Cu–O_2	1.86	0.7	–	–	1.82	0.9
C_xH_y, 773 K	Cu–O_1	–	–	1.98	0.7	1.96	0.9
	Cu–O_2	–	–	1.87	0.6	1.88	1.4
	Cu–Cu	2.52	9.0 (11.2)	2.52	5.3 (10.6)	2.51	2.3 (8.5)
NO/C_xH_y, 773 K	Cu–O_1	1.93	0.6	1.98	1.1	2.00	1.7
	Cu–O_1	–	–	1.86	0.9	1.86	1.3
	Cu–Cu	2.52	8.3	2.52	3.4	2.51	1.3
NO/O_2/C_xH_y, 773 K	Cu–O_1	1.93	3.6	1.95	3.3	1.94	3.4

[a] First coordination shell of Cu in: CuO—4 oxygen atoms at 1.95 Å; Cu_2O—2 oxygen atoms at 1.85 Å; metallic Cu—12 copper atoms at 2.55 Å.

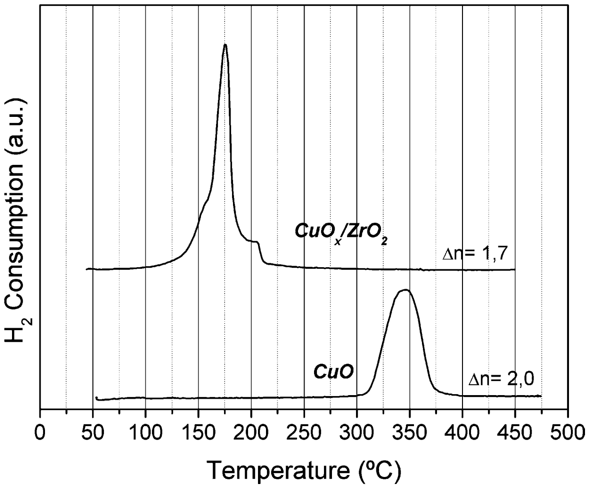

Fig. 7. Temperature-programmed reduction profiles of CuO and a Cu/ZrO_2 catalyst.

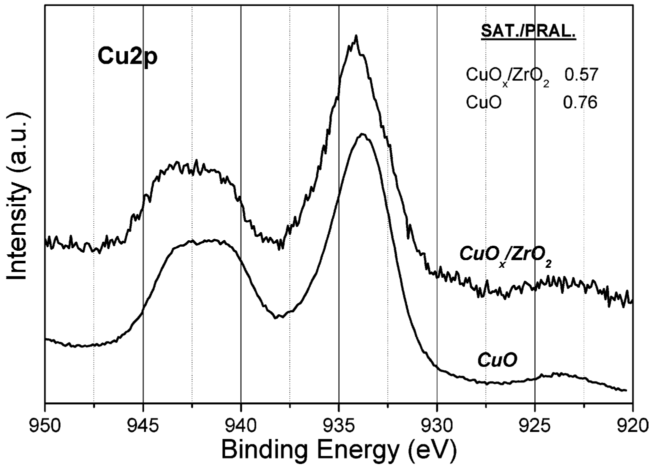

Fig. 8. X-Ray photoelectron spectroscopy of CuO and a Cu/ZrO_2 catalyst.

of copper (I) and (II) oxide phases, which cannot be resolved by conventional fitting analysis. The characteristic coordination numbers for these two phases (4 and 2, respectively) could account for the experimental values included in Table 1.

Additional evidence of the high stability of the copper(I) oxide phase on the zirconia surface can be obtained from TPR and XPS experiments. Fig. 7 shows the reduction profiles obtained for a precalcined CuO_x/ZrO_2 catalyst and a massive CuO sample. Together with the lower temperature range for the reduction of copper in the catalysts, which reveals that this phase was well dispersed on the support, an important difference in hydrogen consumption existed. Although for the massive copper oxide, the hydrogen consumption corresponded to a stoichiometric change from Cu(II) to Cu(0) (i.e., $\Delta n = 2$), for the catalysts, only $\Delta n = 1.7$ was measured. Assuming that only metallic copper was obtained after reduction, a likely explanation for this difference is that some monovalent copper species were present in the calcined catalyst. Although an alternative explanation for this low hydrogen consumption could be that some Cu(II) species were reduced after contact with hydrogen at room temperature before the TPR run, this effect would also provide evidence of the high reducibility of copper dispersed on the zirconia surface. A similar conclusion can be obtained by comparing the XPS of a massive CuO phase with that for a dispersed phase in zirconia (Fig. 8). Cu(II) and Cu(I) species can be easily distinguished by XPS, because the Cu2p signal of the former has a satellite peak centred at a BE of 924 eV, which is not present for Cu(I) [7]. The relative intensity between this peak and the principal one at 934 eV was about 0.76 for the CuO, whereas the highest value obtained for the catalyst was 0.57. This difference, not estimated as relevant in previous XPS results [8], can also supports that the copper in the calcined catalyst is partially reduced, in agreement with the FA analysis of the XANES data.

At this point, it is interesting to stress that although there was relatively good agreement between the fitting results of EXAFS spectra and the FA of the XANES, the FA seems to be more sensitive for detecting low percentages of some components. Thus, although the fitting detected metallic copper only after treatment with propene at 773 K, FA indicated that about 15% of Cu(II) and 5% of Cu(I) were still present in these conditions. These percentages obtained from FA can be alternatively used to obtain more reliable values for the coordination numbers

(CNs) of metallic copper phases as obtained from the fitting analysis of EXAFS spectra. Thus, after reducing treatment with the hydrocarbon at 773 K, the corrected CN for this phase (Table 1) was 11.2 with propene (80% of metallic copper), 10.6 for propane (50% of metal), and 8.5 for methane (27% of metal). This last result also shows that the metallic copper was agglomerated since the start of the reduction process, reaching CN values close to that of massive metal [13]. The reoxidation treatment regenerated the oxidized dispersed phase, as shown by the results from XANES and EXAFS spectra obtained after treatment with the oxidant gas mixture at 773 K. Some Cu(I) species were again stabilized under these oxidizing conditions.

4. Conclusions

In this work, we used the FA technique to analyse XANES spectra of Cu species in Cu/ZrO_2 de-NO_x catalysts subjected to different chemical treatments in situ. FA was previously used by Haller and others [15,16] to analyse XANES spectra. Here, this analysis was done with the first derivative of the spectra. This provided greater accuracy in the calculations and clearer visualisation of well-defined features attributed to Cu^{2+}, Cu^{+}, and Cu^0 species.

The comparison of the XANES/FA results with those obtained by EXAFS showed a good qualitative agreement with respect to the degree of reduction of copper. However, quantitative analysis by fitting of the EXAFS data was not so sensitive in detecting the presence of minority phases clearly evidenced from the FA. By combining these two mathematical methods, we have obtained a more complete vision of the chemical state of the copper in the zirconia catalyst.

From a chemical and catalytic standpoint, our results confirm that propene is the most effective hydrocarbon for reducing copper at high temperature, either alone or in mixtures with NO. At this temperature with a NO/hydrocarbon/O_2 mixture, most copper is as Cu^{2+}, although a not negligible amount (around 10%) is still in the form of Cu^{+}. The presence of this species is interesting, because processes based on Cu^{2+}/Cu^{+} reversible-reduction processes have been proposed as intermediate steps in the reduction of NO with hydrocarbons in combustion exhausts [28].

Acknowledgments

Financial support was provided by the MCyT of Spain (projects 1FD97-0692 and PPQ2001-3108). We thank the ESRF facility and BM29 beamline staff for their experimental support.

References

[1] V.I. Pârvulescu, P. Grange, B. Delmon, Catal. Today 46 (1998) 233.
[2] M.D. Amiridis, T.J. Zhang, R.J. Farrauto, Appl. Catal. B: Environ. 10 (1996) 203.
[3] G. Centi, S. Perathoner, Y. Shioya, M. Anpo, Res. Chem. Intermed. 17 (1992) 125.
[4] V. Indovina, M. Occhiuzzi, D. Pietrogiacomi, S. Tuti, J. Phys. Chem. B 103 (1999) 9967.
[5] S. Bennici, P. Carniti, A. Gervasini, Catal. Lett. 98 (2004) 187.
[6] D. Pietrogiacomi, D. Sannino, A. Magliano, P. Ciambelli, S. Tuti, V. Indovina, Appl. Catal. B 36 (2002) 217.
[7] J.P. Espinós, J.J. Morales, A. Barranco, A. Caballero, J.P. Holgado, A.R. González-Elipe, J. Phys. Chem. B 106 (2002) 6921.
[8] J.J. Morales, A. Caballero, J.P. Holgado, J.P. Espinós, A.R. González-Elipe, J. Phys. Chem. B 106 (2002) 10185.
[9] K. Mathisen, D.G. Nicholson, A.N. Fitch, M. Stockenhuber, J. Mater. Chem. 15 (2005) 204.
[10] A. Bensaddik, A. Caballero, D. Bazin, H. Dexpert, B. Didillon, J. Lynch, Appl. Catal. A. 162 (1997) 171.
[11] G.T. Palomino, S. Bordiga, A. Zecchina, G.L. Marra, C. Lamberte, J. Phys. Chem. B 104 (2000) 8641.
[12] Y.J. Huang, H.P. Wang, J.F. Lee, Chemosphere 50 (2003) 1035.
[13] J.D. Grunwaldt, M. Caravati, S. Hannemann, A. Baiker, Phys. Chem. Phys. 6 (2004) 3037.
[14] J.P. Holgado, J.J. Morales, A. Caballero, A.R. González-Elipe, Appl. Catal. B 31 (2001) L5.
[15] M. Fernandez-Garcia, C. Marquez-Alvarez, G.L. Haller, J. Phys. Chem. 99 (1995) 12565.
[16] M.K. Neylon, C.L. Marshall, A.J. Kropf, J. Amer. Chem. Soc. 12 (2002) 5457.
[17] C.E.M. Campos, J.C. de Lima, T.A. Grande, K.D. Machado, J.P. Itie, A. Polian, J. Solid State Chem. 179 (2005) 93.
[18] A. Bleier, R.M. Cannon, Mater. Res. Soc. Symp. Proc. 73 (1986) 71.
[19] D. Bonin, P. Kaiser, C. Freitigny, J. Desbarres, in: H. Dexpert, A. Michalowizc, M. Verdagner (Eds.), Structures Fines d'Absorption des Rayos X en Chemie, vol. 3. Logiciels d'Analyse EXAFS, Societé Francaise de Chimie, Paris, 1989.
[20] J.J. Rehr, J. Mustre de Leon, S.I. Zabinsky, R.C. Albers, J. Am. Chem. Soc. 113 (1991) 5135.
[21] H. Oguchi, T. Nishiguchi, T. Matsumoto, H. Kanai, K. Utani, Y. Matsumura, S. Imamura, Appl. Catal. A 281 (2005) 69.
[22] C. Palacio, A. Arranz, Surf. Sci. 578 (2005) 71.
[23] M.R. Keenan, P.G. Kotula, Appl. Surf. Sci. 231 (2004) 240.
[24] A.R. González-Elipe, A. Fernández, J.P. Holgado, A. Caballero, G. Munuera, J. Vaccum Sci. Technol. A 11 (1993) 58.
[25] J.P. Holgado, R. Alvarez, G. Munuera, Appl. Surf. Sci. 161 (2000) 301.
[26] Y. Okamoto, T. Kubota, H. Gotoh, Y. Ohto, H. Aritani, T. Tanaka, S. Yoshida, J. Chem. Soc., Faraday Trans. 94 (1998) 3743.
[27] Y. Okamoto, H. Gotoh, Catal. Today 36 (1997) 71.
[28] G.P. Ansell, A.F. Diwell, S.E. Golunski, R.R. Hayes, J.W. Rajaram, T.J. Truex, A.P. Walter, Appl. Catal. B 2 (1993) 81.
[29] R. Burch, S. Scirè, Appl. Catal. B 3 (1994) 295.
[30] Inorganic Crystal Structural Database (ICSD), Fiz Karlsruhe (Germany).